AN ABSTRACT OF THE THESIS OF

Taylor N. Johnson for the degree of Master of Science in

Electrical and Computer Engineering presented on June 11, 2012

Title: Target-Based Coverage Extension of 802.11 MANETs Via Constrained UAV Mobility

Abstract approved: _____

Ben Lee

MANETs are known to be useful in situations where mobile nodes need to communicate and coordinate in dynamic environments with no access to fixed network infrastructure. However, connectivity problems can occur when sub-groups within a MANET move out of communication range from one another. The increasingly prolific use of UAVs in military and civilian contexts suggests that UAVs may be very useful for facilitating connectivity between otherwise disconnected mobile nodes. Network Centric Warfare (NCW) theory makes heavy use of MANETs, and UAVs also fit well into the NCW theory; this paper describes the work involved in integrating network enabled UAVs into a previously-developed simulation of ground troop mobility called UMOMM. Specifically, we created a simple decision model for constrained, constant-radius UAV movements, and developed a target-based method by which UAVs can distribute themselves in order to improve the connectivity of the ground members of the MANET.

Target-Based Coverage Extension of 802.11 MANETs Via Constrained UAV Mobility

by

Taylor N. Johnson

A THESIS

submitted to

Oregon State University

in partial fulfillment of
the requirements for the
degree of

Master of Science

Presented June 11, 2012
Commencement June 2012

Master of Science thesis of Taylor N. Johnson presented on June 11, 2012

APPROVED:

Major Professor, representing Electrical and Computer Engineering

---

Director of School of Electrical Engineering and Computer Science

---

Dean of the Graduate School

I understand that my thesis will become part of the permanent collection of Oregon State University libraries. My signature below authorizes release of my thesis to any reader upon request.

Taylor N. Johnson, Author

ACKNOWLEDGEMENTS

I would first like to thank my advisor, Dr. Ben Lee, for his persistent encouragement and expert guidance during this entire process. I appreciate his earnest interest in my success and growth, and also his ability to foster a collegial environment among his graduate students.

I would also like to thank all of my friends and colleagues in the School of Electrical Engineering & Computer Science, with whom I frequently engage in interesting and useful discussions.

I would also like to thank my parents, my friends, and the rest of my family for their constant support and words of kindness, especially my fiancée Jessica.

TABLE OF CONTENTS

LIST OF FIGURES

TARGET-BASED COVERAGE EXTENSION OF 802.11 MANETS VIA CONSTRAINED UAV MOBILITY

1. INTRODUCTION

Network Centric Warfare (NCW) is a modern theory that focuses on increasing combat effectiveness by linking or networking resources among military forces [1]. At the most basic level, it is about obtaining and maintaining information superiority in a battlefield context, promoting collaboration among ground units, and raising situational awareness in order to increase mission effectiveness [2]. Information superiority is obtained by collecting accurate, detailed, real-time information and distributing it to all levels of command and control. To facilitate the collection of information, future soldiers will be equipped with an integrated set of high-technology devices such as GPS, wireless communication platforms, and sensors. The data obtained from these devices will then be linked to an array of other real-time and archived battlefield information resources.

Figure 1.1 illustrates the basic concept behind the NCW theory. Ground units in the NCW model are partitioned into groups based on a traditional military organizational structure (platoons, squads, etc.), and are deployed into tactical operation areas. While units within a single tactical operation area will generally remain within communications range with one another, inter-communication between tactical operation areas is less likely with only ground units deployed. For this reason, the NCW model includes low altitude, network-enabled *Unmanned Aerial Vehicles* (UAVs), which can act as waypoints between ground units that would otherwise not be able to communicate. The inclusion of low altitude UAVs also has the effect of extending the operational range of NCW ground

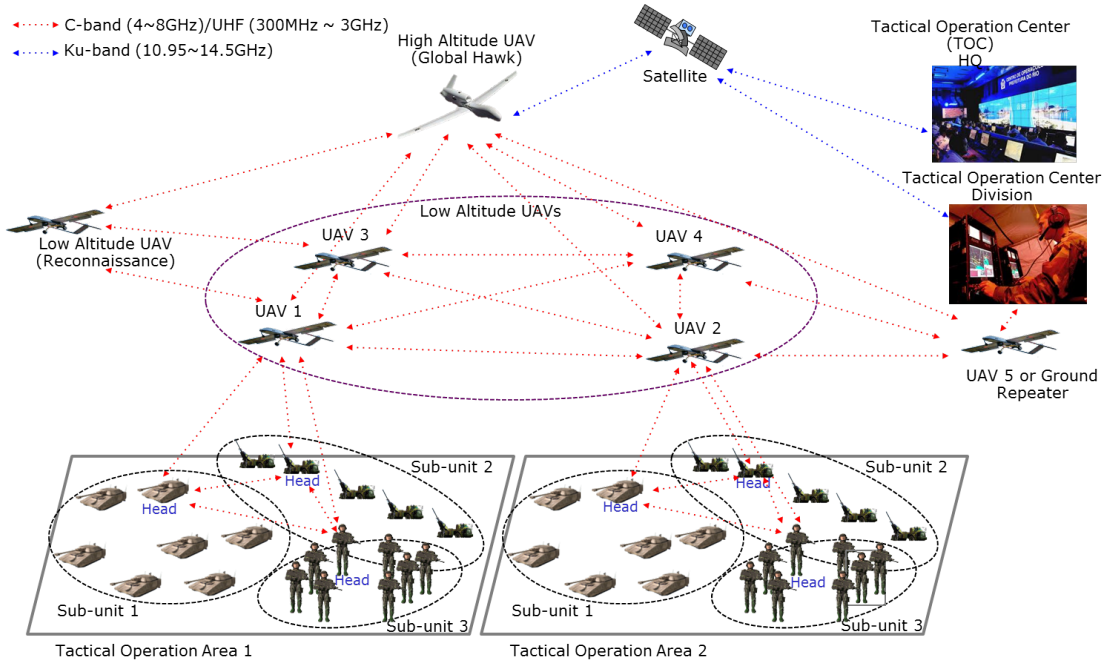

FIGURE 1.1: Conceptual view of Network Centric Warfare theory.

units. Also included in the NCW model is a high altitude UAV (global hawk), which monitors and communicates with the low altitude UAVs. The main role of the high altitude UAV is to relay information received from the low altitude UAVs to a satellite, which in turn relays the information to all relevant command centers, such as the tactical operation center (TOC).

Communication within the NCW model is facilitated via the formation of Mobile Ad-hoc NETworks (MANETs), which are used to provide crucial information, such as videos and pictures of combat situations as well as location and vital signs of soldiers, back to the command structure. MANETs are prevalent within the NCW model because they require no infrastructure or pre-configuration, and thus they can be used to dynamically create communication networks for groups of wireless users in any situation, such as open areas, mountainous regions, and urban areas. In a MANET, the network topology frequently changes based on the movement of mobile nodes, e.g., soldiers. Therefore, routing protocols are crucial for maintaining some degree of connectivity, even as nodes

move. However, the performance of routing protocols has been difficult to evaluate because of lack of mobility models that realistically represent the behavior of mobile nodes in military situations. The previously-developed *Urban Military Operation Mobility Model* (UMOMM) was created in part to provide a platform for the proper evaluation of various routing protocols in the context of MANETs.

Previous research in the field of UAV mobility has generally focused on simplistic reconnaissance and plume detection applications. Many studies are based on small scale trace data. To date, no one has developed a UAV mobility model that specifically fits within the NCW model. Therefore, this thesis presents a UAV mobility model that works together with an NCW-based ground mobility model (UMOMM), in order to evaluate UAV effectiveness in the context of the NCW theory.

2. BACKGROUND & RELATED WORK

Due to the nature of the NCW model, the movement of UAVs is of secondary importance compared to the movement of ground units, which must base their actions solely on the requirements of the mission. Since this implies that UAVs are acting in a strictly supportive role, it is important to first review the previous work concerning the mobility of ground units.

2.1. Ground Mobility

Much work has been done previously regarding basic synthetic mobility models. Generally, mobility models are categorized into two types: *entity mobility* models, where each node moves independently of all other nodes, and *group mobility* models, where nodes move as a group.

A basic, well-studied synthetic entity mobility model is Random WayPoint (RWP) [3], which is commonly used in ad hoc network simulations because of its simplicity. In RWP, each mobile node is randomly assigned a starting location within a simulation area. Next, destinations are randomly selected for each of the nodes, and then each node moves toward its destination with a randomly selected constant velocity. Upon arriving at a destination, a mobile node remains stationary for a pause time, and then moves toward a new waypoint with a new randomly selected velocity. After a certain amount of simulation time for RWP mobile nodes, the node density tends to be very high at the center of the simulation area, and almost zero at the borders [4] [5].

There are many other entity mobility models that are closely related to RWP. Generally, they are distinguished from RWP based on the addition of some constraints on mobility. For example, limiting movement to either streets or highways, or restricting

movement to account for obstacles. Bai et al. introduced the Manhattan Mobility Model and the Freeway Mobility model, both used for simulating movement in a metropolitan area [6]. The Manhattan Mobility Model restricts all node movements to a specified map composed of horizontal and vertical streets, each having two lanes. The Freeway Mobility Model uses a map composed of freeways of several lanes in both directions, where each mobile node travels with some safe distance and velocity relative to the node in front of it. The Graph-based Mobility Model [7] uses the vertices of a graph as locations that mobile nodes can visit, and the edges of the same graph as streets or train connections. The graph itself represents node movements that are restricted by buildings and streets. More recent work places an additional focus on the delays incurred due to stoplights at intersections [8]. Restriction of movement can also exist without the use of roads. For example, in the Obstacle Avoidance Mobility model [9], nodes move from source to destination via the shortest path around a polygonal obstacle.

While RWP and the related mobility models shown were all entity models, there are also many group mobility models that have been suggested and implemented, such as the Reference Point Group Mobility (RPGM) model [10] and the Structured Group Mobility Model (SGMM) [11]. In these models, a mobile node is permanently affiliated with a pre-defined group and the group mobility pattern is fixed to the reference node or a group leader's movement. RPGM considers the spatial relationship and movement behavior among the members of a group: each group is composed of a logical center, called the group leader, and a number of group members. The group leader determines the rest of the group's motion behavior, including location, speed, direction, acceleration, and reference point. SGMM extends RPGM to handle multiple group simulations by applying the model recursively.

The Virtual Track (VT) model [12] supports group partitioning and merging scenarios, and defines a simulation area as switch stations and virtual tracks. The switch

stations are randomly deployed in the simulation area and connected by virtual tracks. The groups are distributed along the virtual tracks and individual nodes are distributed within the simulation area. The groups use the virtual tracks for their movement but the individual nodes can move anywhere as in the RWP model. Partitioning occurs when nodes of the group choose a different switch station, and merging occurs when several groups arrive at the same switch station and decide to use the same virtual track to the next destination.

The Reference Region Group Mobility (RRGM) model [13] also supports group merging and partitioning. Every group is associated with a reference region, an intermediate location or destination where the group will eventually move. When multiple reference regions are assigned to one group, the group will be partitioned into a number of smaller subgroups associated with different destinations. When a subgroup reaches its destination, it could merge with another group if the other group has also arrived at the same destination.

2.2. Prior Work of Ground-UMOMM

There have been many research efforts on synthetic entity and group mobility models that, although useful, cannot be applied in realistic combat operation scenarios. The movements of nodes in a military situation are not independent but typically interrelated, with potentially complex mobility scenarios that depend on the tactical situation. A typical characteristic of military operation is that a group can dynamically partition itself into a number of subgroups or merge with another group. For instance, in urban areas, a number of army units will first mobilize outside the urban area. Once orders are given based on the tactical situation, units then move toward their destinations by navigating the urban environment. During the operation, a group may be divided into several subgroups

where some of the subgroups are assigned new tasks while the rest of the subgroups continue towards their original objectives. After completing the new tasks, subgroups will rejoin the main force.

The previously-developed *Urban Military Operation Mobility Model* (UMOMM) incorporates features from many of the previously developed synthetic mobility models, such as the initial positioning of groups in RPGM, and the graph representation of urban streets first seen in the Graph-based Mobility Model. However, UMOMM is an improvement over previous work for the following reasons:

- While the Manhattan Mobility and Freeway Mobility models use geographic restriction, UMOMM does so in conjunction with a group model. UMOMM recognizes that nodes are often related to each other and can have complex mobility patterns depending on the situation and the composition of military units.

- The VT and RRGM models support group partitioning and merging scenarios, but do not specify the relationship and command structure among groups. If a partition event occurs, the resulting subgroups will have no memory of their previous grouping. UMOMM specifies a command structure as a more realistic model, as the behavior of VT and RRGM is not sufficient for modeling mobility patterns of soldiers in urban areas under dynamically changing situations.

- UMOMM incorporates all three important characteristics of synthetic mobility models: temporal dependence of velocity, geographic restriction of movement, and spatial dependence of velocity.

UMOMM is a good example of an NCW-compliant ground mobility model because of a few unique features: First, UMOMM is a military mobility model for infantry units that are restricted to movement within an urban area. This has become increasingly important for simulating modern battle situations encountered by troops. For a realistic

organizational structure between infantry units, UMOMM adopts a platoon as the basic group type within the model. Platoons can be dynamically partitioned into smaller squads, each with a new task, and then they can be reconstituted later at an arbitrary point along the platoon's route to its destination. The mobility of platoons in UMOMM can also be extended to model the operations of larger military units such as a company, battalion, or division. Second, the mobility characteristics of troops in UMOMM can differ depending on the mission of each platoon. Mission types can include surveillance, gaining control of maneuver routes and intermediate locations, and occupying the assigned locations on the map. UMOMM can also model situations where groups encounter various obstacles constructed by hostile forces, and must overcome them to reach the destination.

2.3. Prior Work on UAV Mobility Models

Although much work has been done concerning UAVs in general, research involving UAV mobility, especially with a focus on studying network connectivity, is somewhat limited. Random movement and obstacle-based models are commonly explored when performing mobility studies [14]. Lu *et al.* developed a UAV mobility model based on trace data generated during a military experiment [15], but did not measure the effects of their mobility model on network connectivity. Testbed implementations have been performed [16][17][18], but they are often of small scale and present difficult-to-replicate results. Simulation studies of UAV mobility have also been performed, but are limited target applications that involve reconnaissance [19] or plume detection [20]. To date, no UAV mobility models have been developed to work in conjunction with a realistic, hierarchical ground mobility model like UMOMM, and no UAV mobility models have attempted to specifically solve the problem of increasing connectivity. The closest attempt occurs in [21], which tries to improve connectivity by adding static nodes to a MANET.

Although several papers have already been written studying the various facets of UAV mobility, their results are generally not useful for application to NCW. However, their results did help steer the development of the integrated UAV/Ground-UMOMM.

Brown *et al.* performed an experimental study using 802.11b radios placed on ground vehicles and UAVs, creating a mobile ad hoc wireless network [22]. A testbed was established for two different scenarios: (1) using a single UAV as a relay between two ground nodes that would otherwise not be able to communicate (such as in Figure 2.1(a)), and (2) using multiple UAVs to relay messages, effectively extending the communication range of all nodes involved (such as in Figure 2.1(b)). The experiment had the following key results:

- With a 1 W radio output, ground-to-ground communications were able to reliably achieve a throughput of around 1 Mbps at distances up to 2 km.
- With a 1 W radio output, ground-to-UAV communications were able to reliably achieve a throughput of around 1 Mbps at distances up to 4 km.
- The addition of a UAV acting as a waypoint drastically improved connectivity between nodes that would otherwise be disconnected, and therefore suffer from gaps in service.

Goddemeier *et al.* compared two UAV steering strategies: self repelling random walk (SRW) and cooperative repelling random walk (CRW), both of which are techniques for covering regions of interest [20]. A self repelling walk is a coverage strategy in which nodes are allowed to revisit previously-encountered nodes with low (but non-zero) probability. A cooperative repelling walk assumes that nodes are aware of the position of other nodes, and are therefore able to avoid the previous locations of all nodes, instead of just themselves. The paper shows that cooperation allows for more effective coverage of the target area, although it requires that nodes be aware of the movement histories of all other nodes,

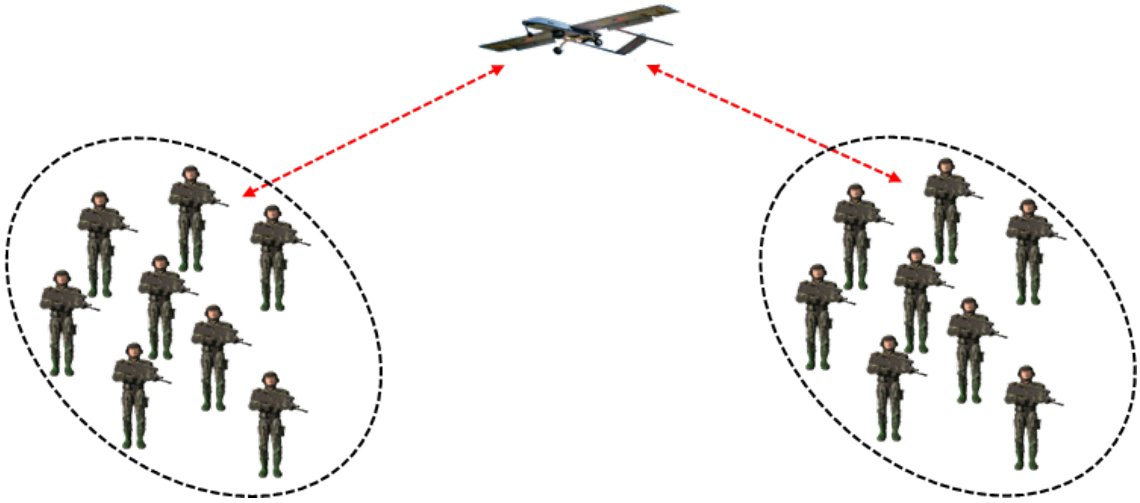

(a) Example of using a UAV to increase connectivity between distant nodes.

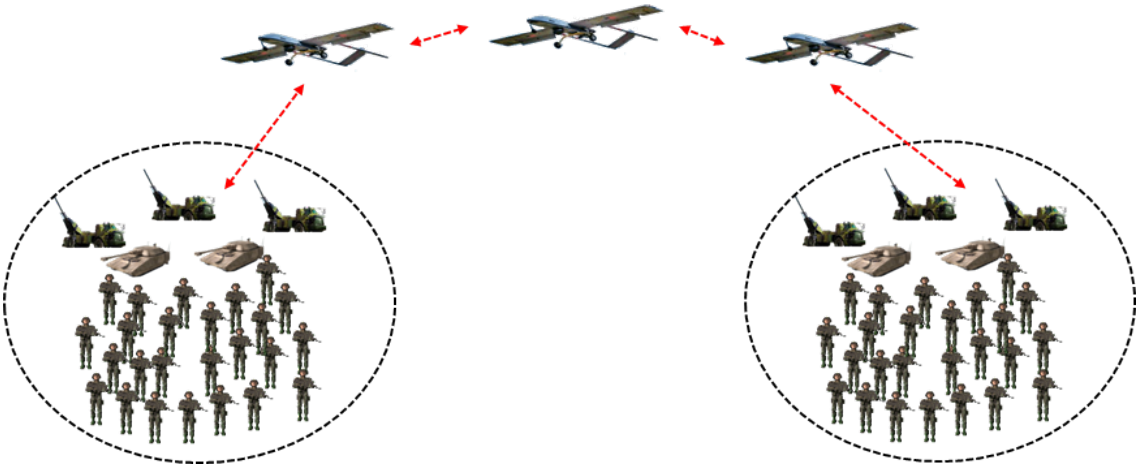

(b) Example of using multiple UAVs to increase the operational range of NCW-enabled nodes.

FIGURE 2.1: Two uses for low-altitude UAVs in NCW theory

which can be a non-trivial requirement under certain situations.

Reich *et al.* introduced the Spreadable Connected Autonomic Network (SCAN) algorithm, which is a method for maintaining connectivity in mobile wireless networks [17]. SCAN uses knowledge of the network topology to make mobile nodes stop their movement before they break the connectivity of the mobile network. While this method appears to be useful for maximizing connectivity, it is not acceptable for UMOMM nodes to artificially

halt in order to maintain a good connection. UMOMM ground units must be able to move freely in order to accomplish their mission; network connectivity is secondary to this requirement.

Kuiper and Nadjm-Tehrani looked at what impact a UAV mobility pattern can have on network performance and connectivity [19]. Specifically, two mobility models were developed to simulate a reconnaissance mission performed by UAVs:

- The first mobility model is a basic random model where the UAVs do not coordinate their movements. In this model, each UAV decides every second whether it should maintain its current direction, turn right, or turn left, and makes these decisions according to a "random action table" of probabilities that also considers the most recent action. This simple mobility model also contains provisions for returning UAVs to the operational area if and when they move outside its borders.

- The second mobility model is a distributed pheromone repel model, where the movement of a UAV during simulation can depend on the movement of other UAVs included in the simulation. In this model, each UAV maintains a map containing a list of positions previously visited, and a list of timestamps indicating when each position was last visited. The UAVs share their map data with one another on a periodic basis, such that all UAVs have a comprehensive, merged map of recently visited locations. Decisions are also made each second in this mobility model; however, instead of consulting a random action table to make a decision about where to move next, each UAV bases its decision on how recently an area has been visited (specifically, each UAV decides to move to the position which has not been visited recently).

The two mobility models presented in this paper were evaluated based on the amount of coverage achieved by 10 UAVs during a two hour simulation. The pheromone model consistently achieved coverage exceeding 90% over the course of 10 simulation runs. The

random model's coverage was generally between 80% and 90%. An interesting result was that both models resulted in a low level of connectivity between nodes during the simulation, suggesting that connectivity suffers when maximal coverage is the singular goal. The authors concluded that there is an "inherent conflict" between the two goals of maximal coverage and maximal connectivity, and that those designing mobility models should be conscious of the fact that prioritizing one goal can often mean sacrificing the other.

Danilov performed a field demonstration that yielded experimental results for network traffic and routing information in a configuration that included UAVs and ground units [18]. Similar to the work in [22], 802.11 radios were installed on two fixed-wing UAVs. One UAV was configured to stream video at 400 Kbps, while the second UAV was available for forwarding (if necessary). Additionally, constant bitrate multicast traffic was introduced during the experiment. The authors noticed that the availability of the second UAV for forwarding of data had a direct effect on the loss rate of multicast packets. In general, more packets were lost when the first UAV had to rely solely on the ground network for communication. Moreover, the authors noticed that wireless link quality varied during the course of the experiment, due to environmental conditions such as change in windspeed or temperature.

Han *et al.* studied smart deployment of UAVs in order to provide communication advantages to ground-based networks [23]. This paper takes a formal approach to maximizing network connectivity, specifying the following four measures of connectivity:

- *Global message connectivity* - the probability of successfully delivering a single message to every node in a mobile ad hoc network.
- *Worst-case connectivity* - a measure of how close a network is to becoming disconnected/divided.
- *Network bisection connectivity* - the cost of dividing the network.

- *k-connectivity* - quantifies how many nodes must fail before the network is disconnected.

The paper shows that, by defining the above measures of connectivity in terms of spanning trees, spectrum graph theory, and max-flow min-cut, finding an optimal solution to the UAV deployment and movement problem is NP-hard. However, heuristic algorithms exist that can approximate an optimal solution with significantly less computational complexity. The paper concludes that "for general network setups, a UAV can improve the global message connectivity and the worst-case connectivity by 109% and 60%, respectively ... network bisection and k-connectivity are also improved by the addition of a UAV to the network".

3. THE PROPOSED UAV MOBILITY MODEL

The primary objective of this paper is to develop a realistic UAV mobility model in the context of NCW. As noted earlier, UAVs in the NCW model play a support role for the ground units operating in one or more tactical operation areas. Since UAVs in principle can be deployed to extend the communications range of the ground units they are supporting, the issue is how should the UAVs position themselves based on where the ground units are located. Suppose we have the following information:

- There are n UAVs available to serve as waypoints for communication between groups of soldiers on the ground.
- The UAVs have information about the current positions of all ground groups.

Given the above information, the problem statement that needs to be solved is essentially: To which coordinates should the UAVs be sent in order to improve the network connectivity of the ground units?

In order to answer this question, the following method is proposed, consisting of a *Constant-Radius Movement Decision* model and *Coverage Selection* model. The Constant-Radius Movement Decision model prescribes how UAVs should move from one coverage location to another without violating the properties of constant-radius movement. The Coverage Selection model decides, based on how many UAVs are available, where each UAV should be placed in order to increase connectivity.

3.1. Constant-Radius Movement Decision Model

Fixed wing aircraft such as UAVs are limited in their movement: they have minimum and maximum airspeeds and cannot make instantaneous changes in either altitude or

direction. As explained in [19], in order to model a realistic flight path, the proposed UAV mobility model must operate within these limitations. UAVs should move at a constant airspeed, maintain a constant altitude, and either move in a straight line or make a constant radius turn to the left or to the right. Since fixed wing aircraft cannot hover in place, the UAVs in this proposed model "stay in one place" by maintaining a *circular holding pattern* around a point-of-interest, or target.

NS-2, the network simulator used to simulate the proposed model, does not support true circular movement. Instead, movement is dictated simply by specifying a destination and speed, at which point NS-2 simulates the node movement from its current location to its target destination in a direct, linear fashion. Thus, UAVs in this mobility model will approximate a circular flight pattern by traversing an n-sided regular polygon. For example, for a polygon with a perimeter of 3000 m, $n = 75$ sides, and a fixed airspeed of 40 m/s, a UAV can move from one polygon vertex to another in exactly 1 second. This means that prescribing a UAV's movement in NS-2 is now a matter of specifying a new destination once a second, always at the fixed airspeed of 40 m/s. The circle that this method approximates would have a radius of $r = 477.60$ m, and a circumference of 3000.85 m.

When a UAV is tasked with moving from one target to another, it must move from its current circular holding pattern into a new circular holding pattern around its new target. Obviously, there are a multitude of ways to move a UAV from one point to another, even when operating in a motion-constrained status, such as constant-radius turns. Inevitably, some transitional flightpaths are less efficient than others. Therefore, a decision model was developed for selecting among three basic flightpaths, which will transition the UAV from one target to another. It is important to note that these transitional flightpaths may not be the absolute shortest paths from one circle to another; instead, these flightpaths are simple, intuitive choices that allow the UAVs to move quickly to a target without

excessive computation of complex flightpaths.

When a UAV is given a new target, the current holding circle in which it resides is partitioned into three arcs. Figure 3.1 shows an example of this partitioning. Depending on which arc the UAV resides in when it is given a new target circle, it can take one of the following three flight paths:

- If the UAV lies within arc A, it will remain on its current holding circle until the first straight path between points a and d, which is tangent to both circles.
- If the UAV lies within arc B, it will again remain on its current holding circle until it reaches the next straight path that is tangent to both circles at points b and e.
- If the UAV lies within arc C, it will turn to the opposite direction at point c, in effect joining a *transitional circle*, via the straight path between the transitional circle and the target circle at points c and f.

Once a decision has been made regarding which transitional flightpath will be used by the UAV, the x- and y-coordinates of the points where the UAV will break from its source holding pattern and join its destination holding pattern are calculated. These points are the endpoints of the specific tangent selected by the decision model, which is used by the UAV to make its transition.

Before the tangent's endpoints can be calculated, the first step is to find θ, which is defined in Figure 3.2 as the angle of the line between the center of the two circles (in radians, from 0 to 2π). For convenience, ϕ is used in Figure 3.2 to indicate noteworthy interior angles.

The following defines θ for the four cases shown in Figure 3.2 as well as special cases:

- Case 1: $x_2 - x_1 > 0$, $y_2 - y_1 \geq 0$

$$\theta = \arctan\left(\frac{y_2 - y_1}{x_2 - x_1}\right)$$

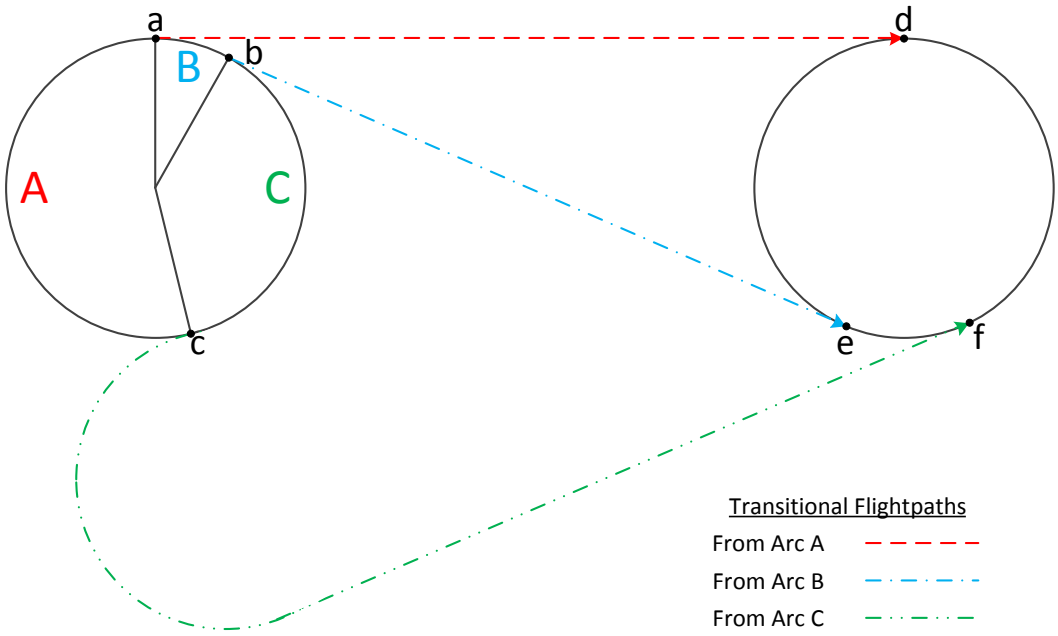

FIGURE 3.1: Decision Model for UAV Transitional Flightpaths. The circle on the left represents the current holding circle and the circle on the right represents the new target circle.

- Case 2: $x_2 - x_1 < 0$, $y_2 - y_1 \geq 0$

$$\theta = \frac{\pi}{2} + \arctan\left(\frac{x_1 - x_2}{y_2 - y_1}\right)$$

- Case 3: $x_2 - x_1 < 0$, $y_2 - y_1 < 0$

$$\theta = \pi + \arctan\left(\frac{y_1 - y_2}{x_1 - x_2}\right)$$

- Case 4: $x_2 - x_1 > 0$, $y_2 - y_1 < 0$

$$\theta = \frac{3\pi}{2} + \arctan\left(\frac{x_2 - x_1}{y_1 - y_2}\right)$$

- Special Cases:

  - If $x_2 - x_1 = 0$ and $y_2 - y_1 > 0$, then $\theta = \frac{\pi}{2}$

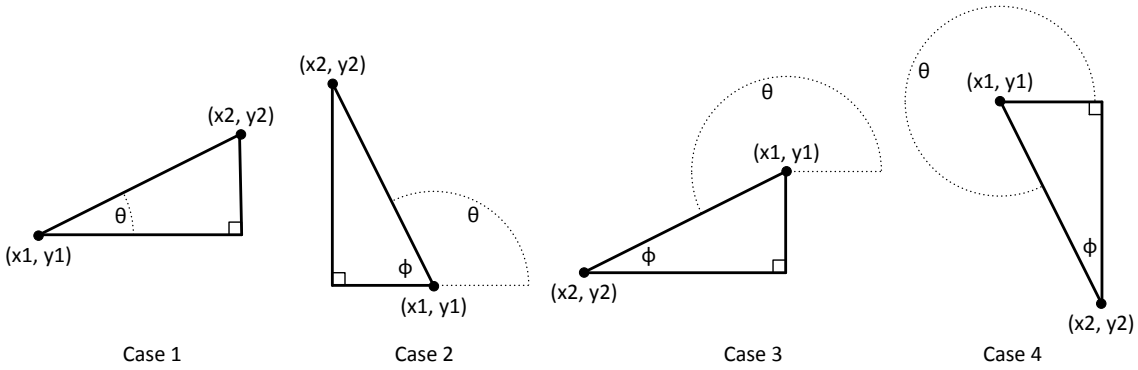

FIGURE 3.2: Illustration of θ for different placements of the circle center points.

- If $x_2 - x_1 = 0$ and $y_2 - y_1 < 0$, then $\theta = \frac{3\pi}{2}$
- If $x_2 - x_1 = 0$ and $y_2 - y_1 = 0$, then the source circle and the destination circle are the same circle, and therefore the UAV is already at its destination.

Once θ has been calculated according to the method described above, the x- and y-coordinates of the end points of the outer tangents can be calculated, which are labelled as $A1$, $B1$, $A2$, and $B2$ in Figure 3.3. The solution to the *Pulley Problem* is useful for finding these coordinates. For example, when the radius is the same for both the source and destination circles (as is always the case in this proposed model), the two outer tangents are parallel to the line between centers of the two circles, and therefore intersect the circles at a $\pi/2$ rotation away (in each direction) from the intersection point of the line between the circle centers.

For Circle 1, if the line segment from the center of the circle to the point $A1$ is treated as a pole with a polar axis in the positive horizontal direction, then the x- and y-coordinates of $A1$ can be calculated using the following polar-to-rectangular conversion:

$$A1_x = x_1 + r \cdot \cos(\theta + \pi/2) \tag{3.1}$$

$$A1_y = y_1 + r \cdot \sin(\theta + \pi/2). \tag{3.2}$$

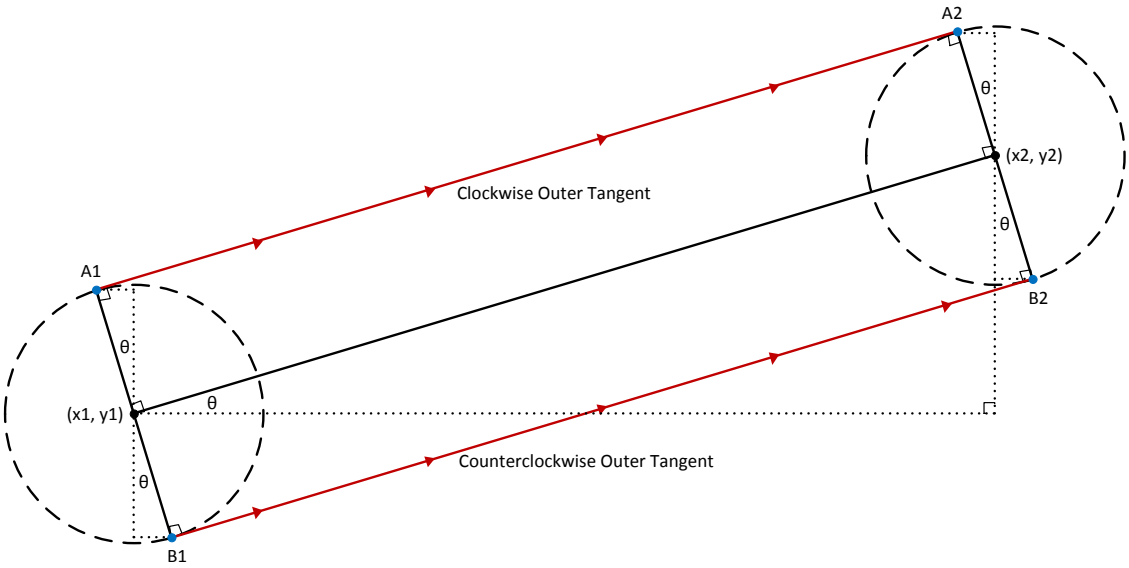

FIGURE 3.3: Example of finding the outer tangents using the *Pulley Problem*.

Calculating $B1$ is another polar-to-rectangular conversion as shown below:

$$B1_x = x_1 + r \cdot \cos(\theta - \pi/2) \tag{3.3}$$

$$B1_y = y_1 + r \cdot \sin(\theta - \pi/2)\,. \tag{3.4}$$

For Circle 2, calculating the coordinates of $A2$ and $B2$ is simply a matter of substituting x_2 for x_1 and y_2 for y_1 in the previous equations.

Knowing θ and r is enough to find the outer tangents, but another piece of information is necessary to find the x- and y-coordinates of the end points of the inner tangents. While the angle between the tangent poles and the line between circle centers is automatically $\pi/2$ for our specific instance of the Pulley Problem, the *Belt Problem* shows that this angle (β in Figure 3.4) varies depending on the distance between the circles, even when both circles have the same r. To find β, the solution to the Belt Problem is used, which is given by:

$$\beta = \arccos\left(\frac{2r}{\sqrt{(x_2 - x_1)^2 + (y_2 - y_1)^2}}\right). \tag{3.5}$$

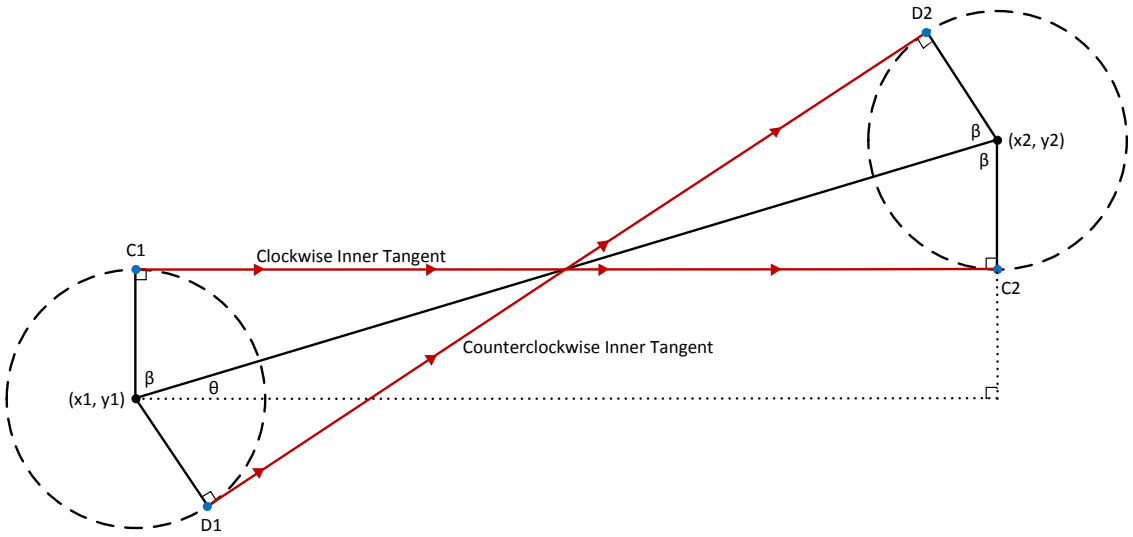

FIGURE 3.4: Example of finding the inner tangents using the *Belt Problem*.

After β, θ, and r are obtained, the x- and y-coordinates of $C1$, $D1$, $C2$, and $D2$ are calculated as follows:

- $C1_x = x_1 + r \cdot \cos(\theta + \beta)$, $C1_y = y_1 + r \cdot \sin(\theta + \beta)$
- $D1_x = x_1 + r \cdot \cos(\theta - \beta)$, $D1_y = y_1 + r \cdot \sin(\theta - \beta)$
- $C2_x = x_2 + r \cdot \cos(\theta + \pi + \beta)$, $C2_y = y_2 + r \cdot \sin(\theta + \pi + \beta)$
- $D2_x = x_2 + r \cdot \cos(\theta + \pi - \beta)$, $D2_y = y_2 + r \cdot \sin(\theta + \pi - \beta)$

It is important to emphasize the distinction between the UAV *holding pattern circle*, which is the actual circular flightpath that the UAV navigates during the course of the simulation, the UAV *instantaneous coverage circle*, which is the area on the ground that the UAV is in communication range with at a given instant, and the UAV *constant coverage circle*, which is the region in the xy-plane that is always within communications range of the UAV, regardless of which portion of the holding circle the UAV currently occupies. Clearly, if increasing connectivity for ground units is our goal, then the constant coverage circle should be as large as possible.

The radius of the holding pattern circle is determined by the flight characteristics of the UAV being modeled. In this proposed model, the radius of all holding circles is 477.60 m. The radius of the instantaneous coverage circle is determined by the maximum transmission range of the UAV, and the UAV's altitude. The radius of the constant coverage circle is the difference between the other two radius values: specifically, $r_{constant} = r_{instantaneous} - r_{holding}$. If $r_{holding}$ is greater than $r_{instantaneous}$, then we end up with the undesirable scenario where no area on the ground is in constant contact with the UAV, and the communication area over times takes on a "donut" shape as portrayed in Figure 3.5.

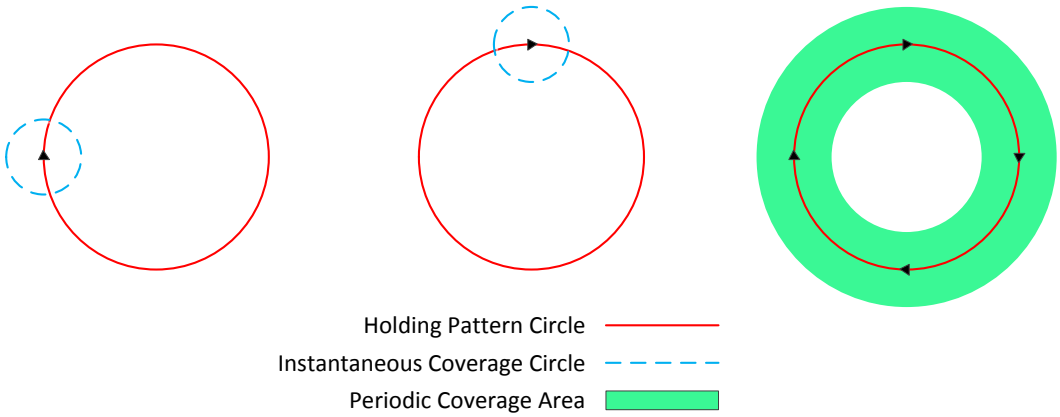

FIGURE 3.5: Example of when the holding pattern circle is larger than the instantaneous coverage circle.

3.2. Coverage Selection Decision

The main problem that needs to be solved is: where should the UAVs be positioned in order to successfully improve the network conditions of the ground troops? Figure 3.6 shows a possible progression of UAV coverage throughout a simulation, where dots represent ground units, rectangles represent clusters of group units, and circles represent coverage areas of UAVs. In Step 1, a single UAV is deployed to a coverage circle that is

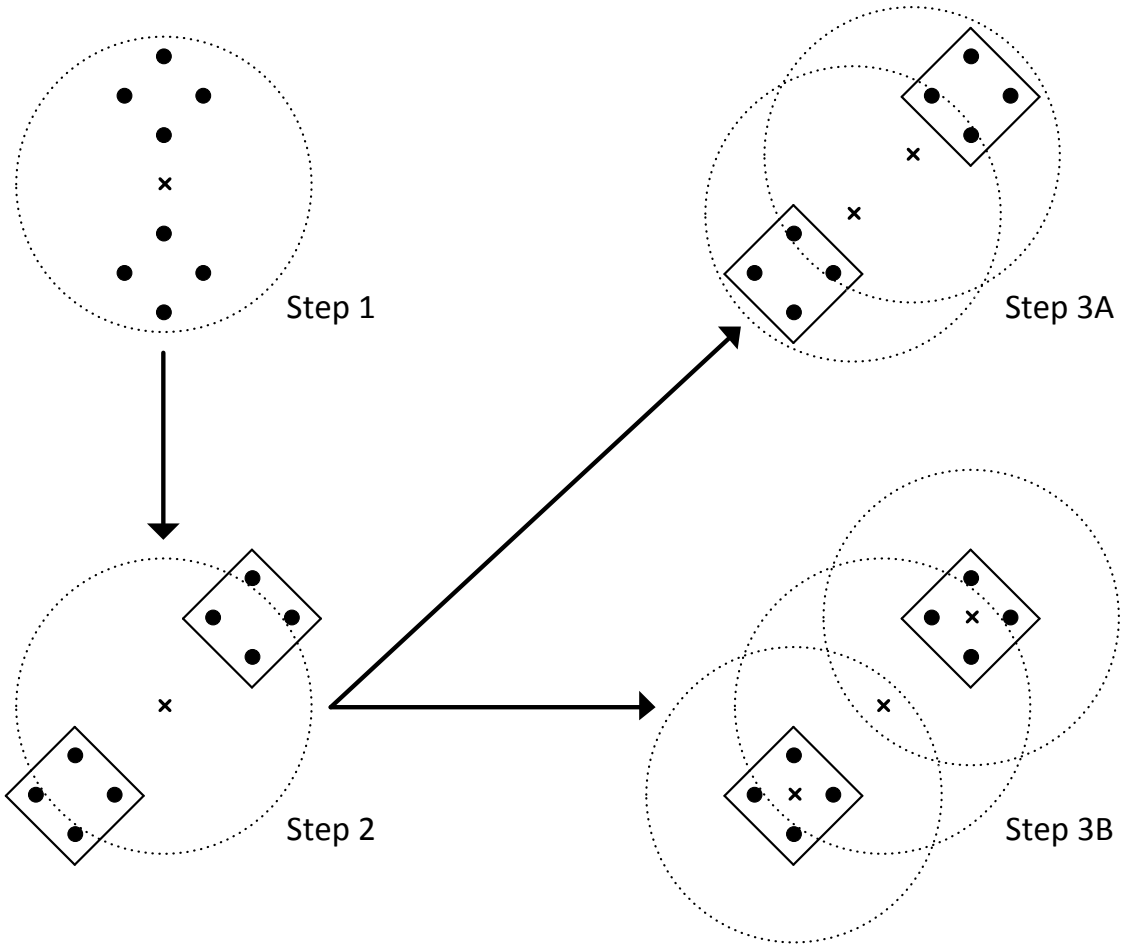

FIGURE 3.6: An example of the coverage circle selection when ground nodes move out of range.

centered at the arithmetic mean of the x- and y-coordinates of all ground units. In this example, the coverage circle of the single UAV is large enough to cover all of the deployed ground nodes, so the UAV will maintain a holding pattern in its coverage circle for as long as all ground units stay within range.

In Step 2, some of the grounds units have moved from their Step 1 positions, such that the single UAV is no longer able to provide coverage to all ground nodes. As a result, the ground nodes are partitioned into *clusters* according to the following criteria: (1) minimize the number of partitions, (2) nearby nodes should generally be clustered

together, and (3) the distance between the furthest nodes in a single cluster must be less than the diameter of a UAV coverage circle. After this partitioning takes place, there are two possible next steps to reestablish full connectivity between ground units. Step 3A favors having a smaller number of UAVs deployed, at the expense of being less robust.[1] On the other hand, Step 3B favors having a robust coverage area, at the expense of requiring more UAVs than Step 3A.

In Step 3A, a second UAV is deployed, and the two UAVs now present in the simulation are placed into coverage circles which are centered at points equidistant from one another and the "center" of each cluster. If this positioning does not result in full connectivity, then additional UAVs are added as needed. In Step 3B, two additional UAVs are deployed, resulting in a total of three UAVs deployed in the operational area. Two of the UAVs are placed into coverage circles located at the "center" of each cluster, and the third UAV is placed directly between the other two UAVs. If the distance between UAVs is such that they are unable to communicate, then additional UAVs are added as needed.

The coverage selection decisions described in this section turn out to be best-suited for scenarios where the number of UAVs in the simulation area can change through out the course of the simulation. However, our work is primarily concerned with the scenario where there is a fixed number of UAVs. The mobility model described in the next section provides more details.

3.3. Mobility Model

After developing a decision model for realistic circular movement of UAVs, the next step is to come up with a way to determine where the holding circles of the UAVs in the simulation should be positioned in order to successfully improve the network conditions of

[1]Robustness is defined in our scenario as the minimum distance that the ground nodes must move before a disconnection event occurs.

the ground troops. UAVs are initially positioned at time 0 in a random location within a 500 $m\times$ 500 m "buffer zone", which is outside of the area where ground troops can exist. The positions of all UAVs after time 0 are dictated by the following mobility model.

The mobility model developed and implemented is based on *k-means clustering*, which is an algorithm that partitions a collection of n points (in our case, the points represent the coordinates of UMOMM ground troops) into k clusters based on the relative distances between points. In other words, points that are close together will be optimally be placed in the same cluster, while points that are far apart will be placed into different clusters. For our application, how many UAVs will be placed in our simulation is first decided, and then k is set to be equal to the number of UAVs. One of the outputs of k-means clustering is a set of k centroids, which represent the geometric centers of the k clusters. These k centroid values are used as the coordinates of the holding circles of the k UAVs in the simulation. The basic algorithm for determining where UAVs should position their holding pattern circles throughout the simulation is as follows:

```
for (every 240 seconds) do
    Collect coordinates of all ground nodes
    Perform k-means clustering on ground node positions (k = # of UAVs), creating
    clusters c_1 to c_k
    for (each UAV i) do
        Assign i's new target as the center of cluster c_i
    end for
end for
```

Each time the UAVs have their target holding circle centers updated, they will immediately begin transitioning to their new destination using the flightpath from the decision model described in Section 3.1.

4. SIMULATION ENVIRONMENT & IMPLEMENTATION DETAILS

The original, ground-only version of UMOMM was developed to work with the NS-2 simulator without modification. However, UAVs pose a different set of challenges, and several additional steps must be taken in order to allow the proposed UAV model to work with the existing UMOMM model and simulated within NS-2. They are *3D Propagation model* and *Long-Range WiFi model*. Each of these models are described in more detail in the following two subsections. This is followed by a description of the parameters needed to properly perform simulation studies.

4.1. 3D Propagation Model

NS-2 provides a free space propagation model that assumes there is a single line-of-sight path from transmitter to receiver, and calculates the received signal power P_r according to the following equation:

$$P_r(d) = \frac{P_t G_t G_r \lambda^2}{(4\pi)^2 d^2 L}, \tag{4.1}$$

where P_t is the transmitted signal power, G_t is the transmitter antenna gain, G_r is the receiver antenna gain, λ is the signal wavelength, d is the linear distance between transmitter and receiver antennas, and L is the system loss. By default, $G_t = G_r = 1$ and $L = 1$.

NS-2 also provides a two-ray ground reflection propagation model that assumes there are two paths from transmitter to receiver; specifically, a direct path and a ground reflection path. For this model, the received signal power P_r is calculated according to the following equation:

$$P_r(d) = \frac{P_t G_t G_r h_t^2 h_r^2}{d^4 L}, \tag{4.2}$$

where d, P_t, G_t, G_r, and L represent the same quantities as in Eq. 4.1, h_t is the height of the transmitter antenna, and h_r is the height of the receiver antenna.[2] $G_t = G_r = 1$ and $L = 1$ are again selected as defaults by NS-2.

The two-ray model is known to be less accurate than the free space model over short distances, so NS-2 uses the free space model for short distances even when the two-ray model is selected during simulation configuration. The distance at which the two-ray model becomes acceptably accurate is known as the *cross-over distance*, d_c. The cross-over distance is the point where the free space model and the two-ray model give the same P_r result. When $d < d_c$, the free space model is used, while the two-ray model is used when $d > d_c$. The cross-over distance is calculated as follows:

$$d_c = \frac{4\pi h_t h_r}{\lambda}. \tag{4.3}$$

Although the free space and two-ray ground reflection models are provided by default with NS-2, the latter does not work properly for communication between nodes that are positioned at different heights, such as a ground unit communicating with a UAV. This is based on the assumptions that the simulation area is completely flat and all nodes are positioned on the ground. Therefore, if NS-2 detects that the nodes attempting to communicate are positioned at different heights, it concludes that the ground is not actually flat and therefore the two-ray model will yield invalid results. In order to accommodate nodes that are not positioned on the ground, NS-2 was modified to remove this false conclusion. With this modification, when nodes are positioned at different heights, it simply means that one of the nodes is a UAV, and the two-ray model will still model signal propagation.[3]

[2]Transmitter and receiver antenna heights are not the same as node heights in NS-2. By default, antennas are located 1.5 meters above their corresponding nodes. This has the effect of ensuring that P_r does not end up as 0 at all distances when the transmitter and/or receiver nodes are located on the ground.

[3]Two-ray propagation modeling could be considered simplistic compared to other existing radio wave propagation models that take into account various physical atmospheric phenomena such as diffraction. However, there are two compelling reasons for its use in our simulation study: (1) two-ray modeling is already implemented in NS-2 for 2D node positions and is easily extended to support 3D node positions, and (2) the ground-only UMOMM simulation study used two-ray modeling.

4.2. Long-Range Wi-Fi

The default maximum communication range between wireless nodes in NS-2 is 250 m, but UAVs and ground leaders in our model need to communicate over distances of up to 2 km. As a result, a number of changes must be made to the default parameter settings of NS-2, specifically in regards to overcoming the limitations on communication distance imposed by the PHY layer and MAC layer models. The PHY layer limitations are easily overcome; as the previous subsection on propagation indicates, increasing the maximum communication distance is simply a matter of changing the transmitted signal power P_t such that the received signal power P_r is greater than the minimum reception power threshold set by NS-2.

The MAC layer limitations require a more detailed analysis in order to be overcome. The default maximum range of 250 m corresponds to a propagation delay of 833.33 ns, based on the NS-2 equation distance/speed-of-light for propagation delay. However, a maximum range of 2 km yields a significantly higher propagation delay:

$$\frac{2000\ m}{300000000\ m/s} = 6.66\ \mu s \tag{4.4}$$

The 802.11 DCF specification does not mention distance limits, but it does assume that the propagation delay has a maximum value of 1 μs. Simó-Reigadas *et al.* demonstrated that delays much greater than 1 μs result in a severe drop in throughput due to ACK frames consistently arriving too late, and they have developed a model for optimizing the 802.11 DCF for long-distance links that illustrates how adjustments to $ACKTimeout$, $CTSTimeout$, $SlotTime$, and CW_{min} can improve performance [24]. To ensure an acceptable level of performance for UAV communication in our model, considered changing these 802.11 DCF parameters in NS-2 according to the recommendations provided in [24]. However, the distance where it becomes truly worthwhile to make MAC timing changes is actually around 5 km, so we decided to keep NS-2's default MAC settings.

5. SIMULATION RESULTS

In order to verify the correctness and effectiveness of our proposed mobility model, a series of simulations was run where UAVs were introduced into Ground-UMOMM simulations. The following list shows which parameters/settings were used to generate our results:

- Number of ground units = 27/54/108 (2/4/6 platoons)
- Number of UAVs = 6
- UAV altitude = 1.75 km
- UAV communication range = 2.00 km
- UAV holding pattern circle radius = 477.60 m
- UAV airspeed = 40 m/s
- Traffic generation from individual members to leaders = 8 KB every 120 s
- Traffic generation from leaders to battalion commander = 12 KB every 1 s

In order to analyze the results, information about ground node positions, UAV positions, packet delivery ratio, and average end-to-end delay was gathered.

5.1. Original UMOMM Parameters

The network performance results shown in Figure 5.1 show that, when the original Ground-UMOMM movement scenario is used with a map that generally keeps the ground units spaced close together, the inclusion of UAVs has no noticeable effect on network performance. UAVs have no measurable effect in this scenario due to a ground unit

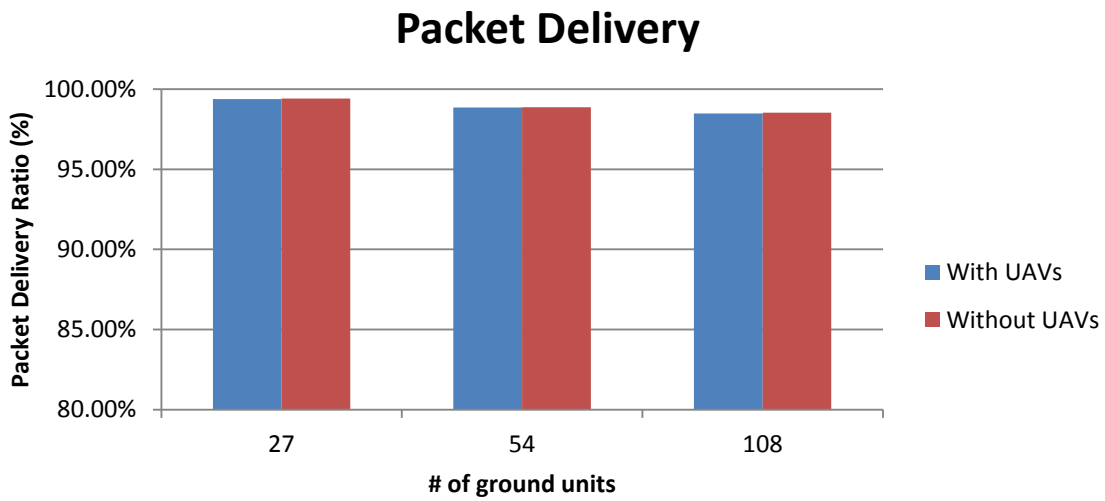

(a) Packet delivery ratio results.

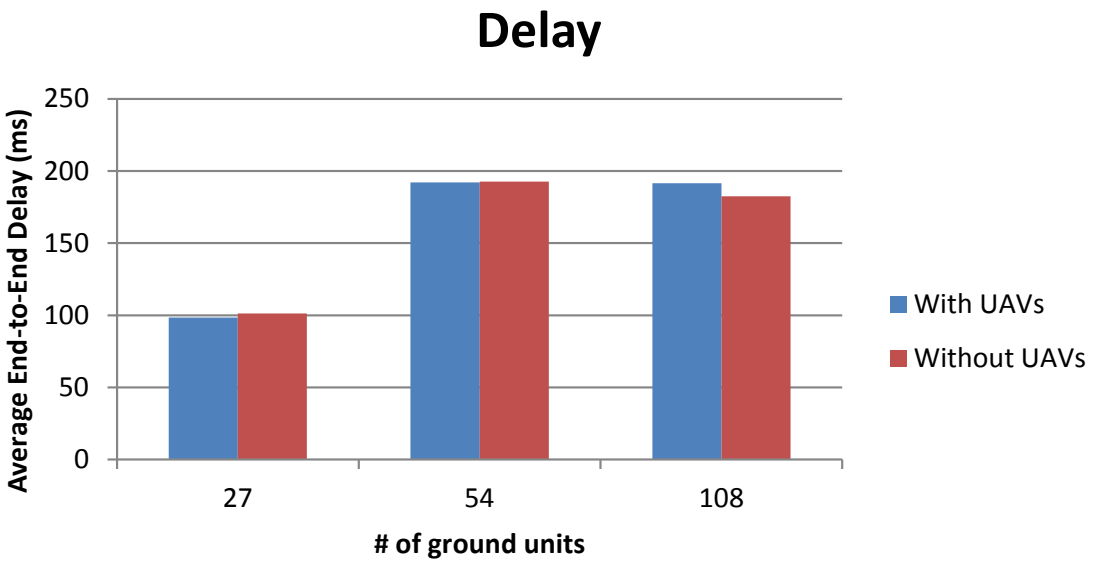

(b) End-to-end delay results.

FIGURE 5.1: Results for simulation with original UMOMM parameters.

spacing which cannot take advantage of UAVs as bridges (i.e., communication between ground nodes is never routed through UAVs because the ground nodes are always within the 250 m communication range).

The results from the original Ground-UMOMM movement parameters *are* able to showcase that the Coverage Selection Decisions are functioning correctly, however. Figure 5.2 shows a trace of the roads used in the 54-ground-unit case during simulation.

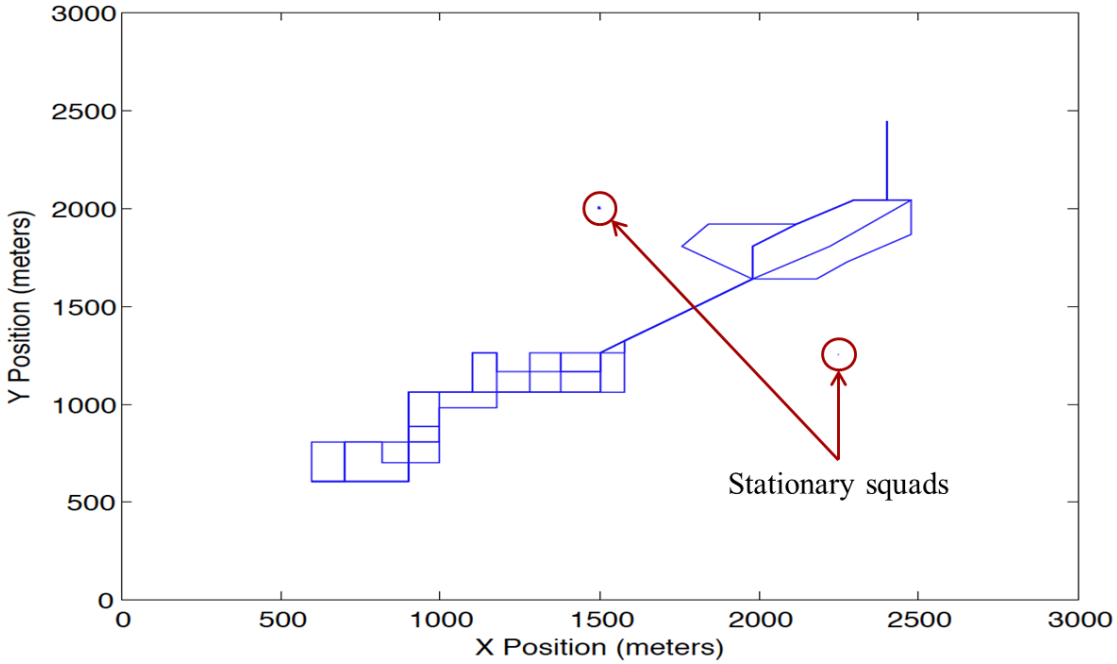

FIGURE 5.2: A trace of the roads traversed by ground units throughout the course of the 54 node simulation run.

Two stationary squads were also included in this simulation run to more effectively showcase the ability of the UAVs to move according to the positioning of ground nodes. Figure 5.3 shows the position of circle centers as determined by k-means clustering, at multiple timestamps. By viewing Figures 5.2 and 5.3 together, it is clear that the locations of UAV holding circles follow the path(s) taken by ground nodes throughout the simulation. This affirms the fact that UAVs are successfully updating the locations of their holding pattern circles based on the positions of ground nodes during the simulation.

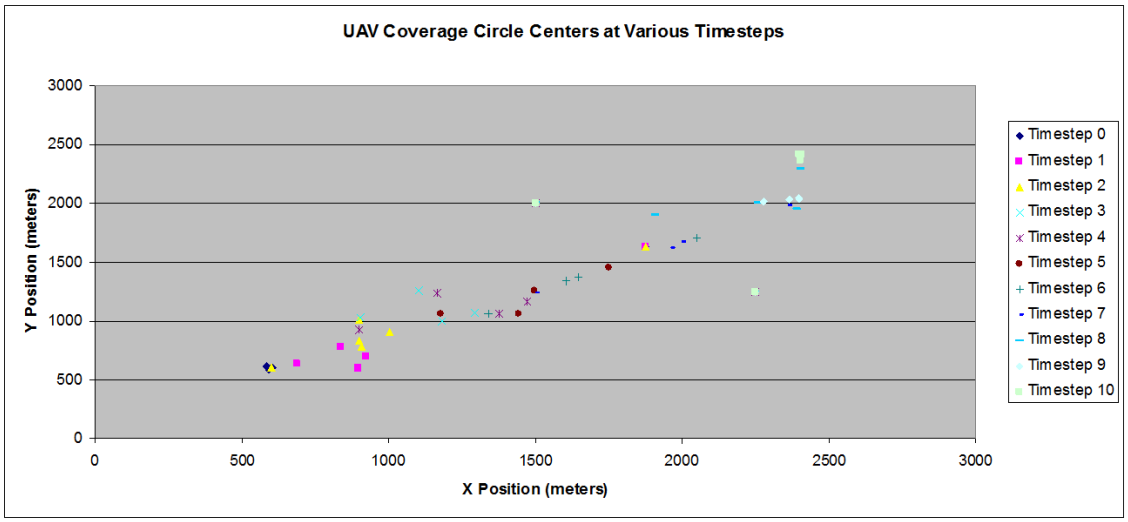

FIGURE 5.3: The positioning of coverage circle centers at each timestep, as determined by k-means clustering

6. CONCLUSION AND FUTURE WORK

Presently, the only way to see the impact of UAVs on network performance is to artificially distort the original UMOMM parameters. This simply means that the original UMOMM model is not the best vehicle to showcase the effectiveness of the proposed UAV mobility model. However, if the Ground-UMOMM units are deployed on an "artificial" map where disconnection events were more prominent, UAVs do have an overall positive impact on the connectivity of ground units. However, this increase in connectivity also results in an increase in overall delay, which could be viewed as a negative side effect when considering that the ground units are meant to be communicating real-time data such as audio and video.

In order to further explore the effectiveness of the proposed UAV mobility model, the future plan is to explore the following issues:

- Analyze the effect of UAVs on network performance with different ground movements scenarios.
- Gather results from multiple routing protocols.
- Gather a wider variety of performance measurements, including routing load, average throughput, etc.
- Develop a metric for measuring the effectiveness of maintaining connectivity.
- Analyze the impact of hidden node and carrier-sense interference.
- Implement advanced UAV techniques (such as having the # of UAVs be adaptive instead of static).
- Use real multimedia data (VoIP, simple video) in simulations, instead of CBR, and measure the effect of UAVs on quantitative & perceptual quality.

Another way to extend this work would be to model the scenario depicted in Figure 2.1(b). Although this type of communication can technically occur in our current scenarios, it is unlikely to occur. For example, suppose a group of ground units is positioned at a location A, and another group is positioned at location B which is 3 km away, and there are four UAVs available. If k-means clustering is simply applied using only the positions of the units at A and B, then two UAVs will be deployed near group A, and two UAVs will be deployed near group B, but the groups will still be unable to communicate with one another. One possible solution to this issue would be to add additional "dummy" position data into the *k-means clustering* algorithm, such that the resulting partition will place the four UAVs in a more beneficial arrangement. This is likely to be an important issue to study in future work.

BIBLIOGRAPHY

1. J. Lyons, S. Swindler, and J. White, "Network centric warfare: Organizational collaboration as a key enabler," in *Collaborative Technologies and Systems, 2008. CTS 2008. International Symposium on*, May 2008, pp. 367 –374.

2. U. S. D. of Defense. CCRP., "Network centric warfare report to congress," 2001. [Online]. Available: http://www.dodccrp.org/files/ncw_report/report/ncw_main.pdf

3. D. Johnson and D. Maltz, "Dynamic source routing in ad hoc wireless networks," *Mobile Computing, T. Imielinski and H. Korth, Eds. Norwell : Kluwer*, vol. 353, pp. 153–181, 1996.

4. E. Royer, P. Melliar-Smith, and L. Moser, "An analysis of the optimum node density for ad hoc mobile networks," in *Communications, 2001. ICC 2001. IEEE International Conference on*, vol. 3, 2001, pp. 857–861.

5. C. Bettstetter, "Mobility modeling in wireless networks: categorization, smooth movement, and border effects," *SIGMOBILE Mob. Comput. Commun. Rev.*, vol. 5, no. 3, pp. 55–66, July 2001.

6. F. Bai, N. Sadagopan, and A. Helmy, "The important framework for analyzing the impact of mobility on performance of routing protocols for adhoc networks," *Ad Hoc Networks*, Jan. 2003.

7. J. Tian, J. Haehner, C. Becker, I. Stepanov, and K. Rothermel, "Graph-based mobility model for mobile ad hoc network simulation," in *Proceedings of the 35th Annual Simulation Symposium*, Mar. 2002, p. 337.

8. D. Gaikwad and M. Zaveri, "A novel mobility model for realistic behavior in vehicular ad hoc network," in *Computer and Information Technology (CIT), 2011 IEEE 11th International Conference on*, Sept. 2011, pp. 597–602.

9. Y. Chenchen, L. Xiaohong, and Z. Dafang, "An obstacle avoidance mobility model," in *Intelligent Computing and Intelligent Systems (ICIS), 2010 IEEE International Conference on*, vol. 3, Oct. 2010, pp. 130–134.

10. X. Hong, M. Gerla, G. Pei, and C.-C. Chiang, "A group mobility model for ad hoc wireless networks," in *Proceedings of the 2nd ACM international workshop on Modeling, analysis and simulation of wireless and mobile systems*, Aug. 1999.

11. K. Blakely and B. Lowekamp, "A structured group mobility model for the simulation of mobile ad hoc networks," in *Proceedings of the second international workshop on Mobility management & wireless access protocols*, Jan. 2004, pp. 111–118.

12. B. Zhou, K. Xu, and M. Gerla, "Group and swarm mobility models for ad hoc network scenarios using virtual tracks," in *Military Communications Conference, 2004. MILCOM 2004. 2004 IEEE*, vol. 1, Nov. 2004, pp. 289–294.

13. J. Ng and Y. Zhang, "Reference region group mobility model for ad hoc networks," in *Wireless and Optical Communications Networks, 2005. WOCN 2005. Second IFIP International Conference on*, Mar. 2005, pp. 290–294.

14. A. Jardosh, E. M. Belding-Royer, K. C. Almeroth, and S. Suri, "Towards realistic mobility models for mobile ad hoc networks," in *Proceedings of the 9th annual international conference on Mobile computing and networking*, ser. MobiCom '03. New York, NY, USA: ACM, 2003, pp. 217–229. [Online]. Available: http://doi.acm.org/10.1145/938985.939008

15. X. Lu, Y.-C. Chen, I. Leung, Z. Xiong, and P. Liò, "A novel mobility model from a heterogeneous military manet trace," in *Proceedings of the 7th international conference on Ad-hoc, Mobile and Wireless Networks*, ser. ADHOC-NOW '08. Berlin, Heidelberg: Springer-Verlag, 2008, pp. 463–474. [Online]. Available: http://dx.doi.org/10.1007/978-3-540-85209-4_37

16. E. Frew and T. Brown, "Airborne communication networks for small unmanned aircraft systems," *Proceedings of the IEEE*, vol. 96, no. 12, pp. 2008 –2027, dec. 2008.

17. J. Reich, V. Misra, D. Rubenstein, and G. Zussman, "Connectivity maintenance in mobile wireless networks via constrained mobility," in *INFOCOM, 2011 Proceedings IEEE*, april 2011, pp. 927 –935.

18. C. Danilov, T. Henderson, T. Goff, J. Kim, J. Macker, J. Weston, N. Neogi, A. Ortiz, and D. Uhlig, "Experiment and field demonstration of a 802.11-based ground-uav mobile ad-hoc network," in *Military Communications Conference, 2009. MILCOM 2009. IEEE*, Oct. 2009, pp. 1 –7.

19. E. Kuiper and S. Nadjm-Tehrani, "Mobility models for uav group reconnaissance applications," in *Wireless and Mobile Communications, 2006. ICWMC '06. International Conference on*, july 2006, p. 33.

20. N. Goddemeier, S. Rohde, and K. Daniel, "Team Interactive Communication and Coverage Strategies for Aerial Plume Detection," in *IEEE/RSJ IROS 2010 Workshop on Robotics for Environmental Monitoring*, 2010.

21. M. Romoozi, S. Vahidipour, and H. Babaei, "Improvement of connectivity in mobile ad hoc networks by adding static nodes based on a realistic mobility model," in *Machine Vision, 2009. ICMV '09. Second International Conference on*, dec. 2009, pp. 138 –142.

22. T. Brown, B. Argrow, C. Dixon, and S. Doshi, "Ad hoc uav ground network (augnet)," in *Proc. AIAA 3rd "Unmanned Unlimited" Technical Conference*, 2004.

23. Z. Han, A. Swindlehurst, and K. Liu, "Optimization of manet connectivity via smart deployment/movement of unmanned air vehicles," *Vehicular Technology, IEEE Transactions on*, vol. 58, no. 7, pp. 3533 –3546, Sept. 2009.

24. J. Simo Reigadas, A. Martinez-Fernandez, J. Ramos-Lopez, and J. Seoane-Pascual, "Modeling and optimizing ieee 802.11 dcf for long-distance links," *Mobile Computing, IEEE Transactions on*, vol. 9, no. 6, pp. 881 –896, June 2010.